Science Advances
AAAS

Supplementary Materials for

Maintaining hypoxia environment of subchondral bone alleviates osteoarthritis progression

Hao Zhang *et al.*

Corresponding author: jingy4172@shu.edu.cn; Xiao Chen, sirchenxiao@126.com; drsujiacan@163.com

Sci. Adv. **9**, eabo7868 (2023)
DOI: 10.1126/sciadv.abo7868

The PDF file includes:

Other Supplementary Material for this manuscript includes the following:

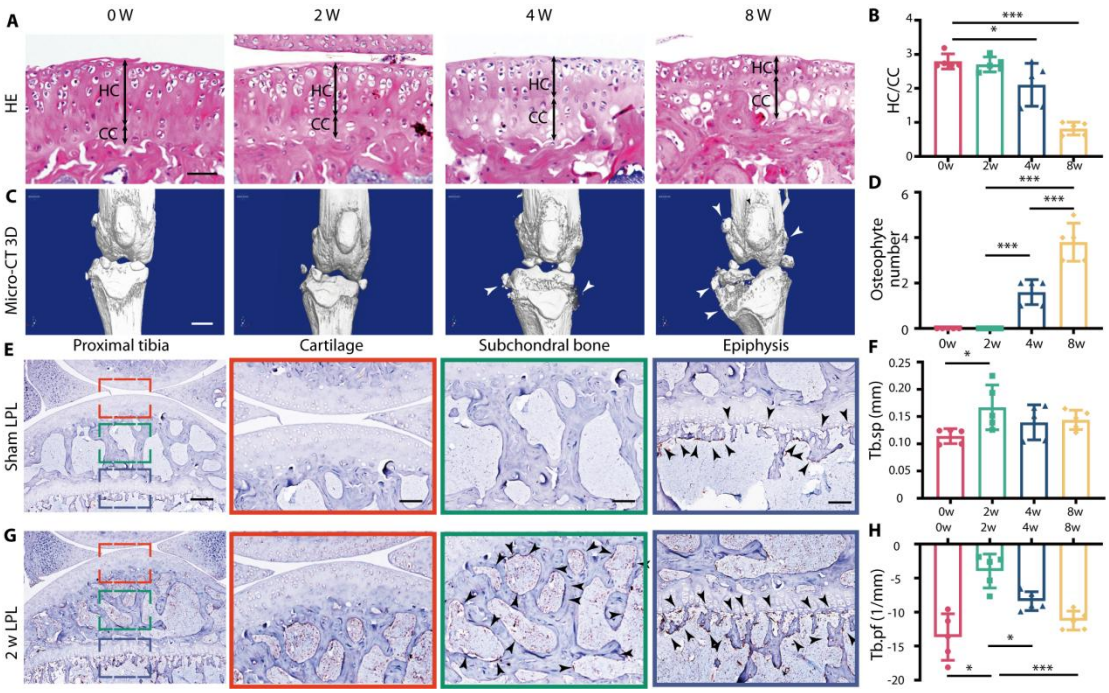

Fig. S1. Establishment of OA models and L-plastin positive cells distribution.

(A) Representative images of Hematoxylin and eosin staining of proximal tibia articular cartilage at 0,2,4 and 8 weeks after ACLT. Double-headed arrows label range of HC and CC. Scale bar, 50 μm. **(B)** Ratio of HC and CC thickness. **(C)** 3D reconstruction of the whole knee joint at 0, 2, 4 and 8 weeks after ACLT. Scale bar, 1 mm. **(D)** Micro-CT quantitative analysis of knee, osteophyte number. **(E)** Representative images of LPL immunohistochemistry in whole normal proximal tibia, articular cartilage, subchondral bone, and epiphysis. **(F)** Micro-CT quantitative analysis of tibial subchondral bone, subchondral bone trabecular separation (Tb.sp, mm). **(G)** Representative images of LPL immunohistochemistry in whole proximal tibia, articular cartilage, subchondral bone, and epiphysis 2 weeks after ACLT. Scale bar, 100 μm (first column). Scale bar, 50 μm (2-4 column). **(H)** Micro-CT quantitative analysis of tibial subchondral bone, subchondral bone trabecular bone pattern factor (Tb.pf, 1/mm). N=5 per group. *P < 0.05 **P < 0.01, and ***P < 0.001.

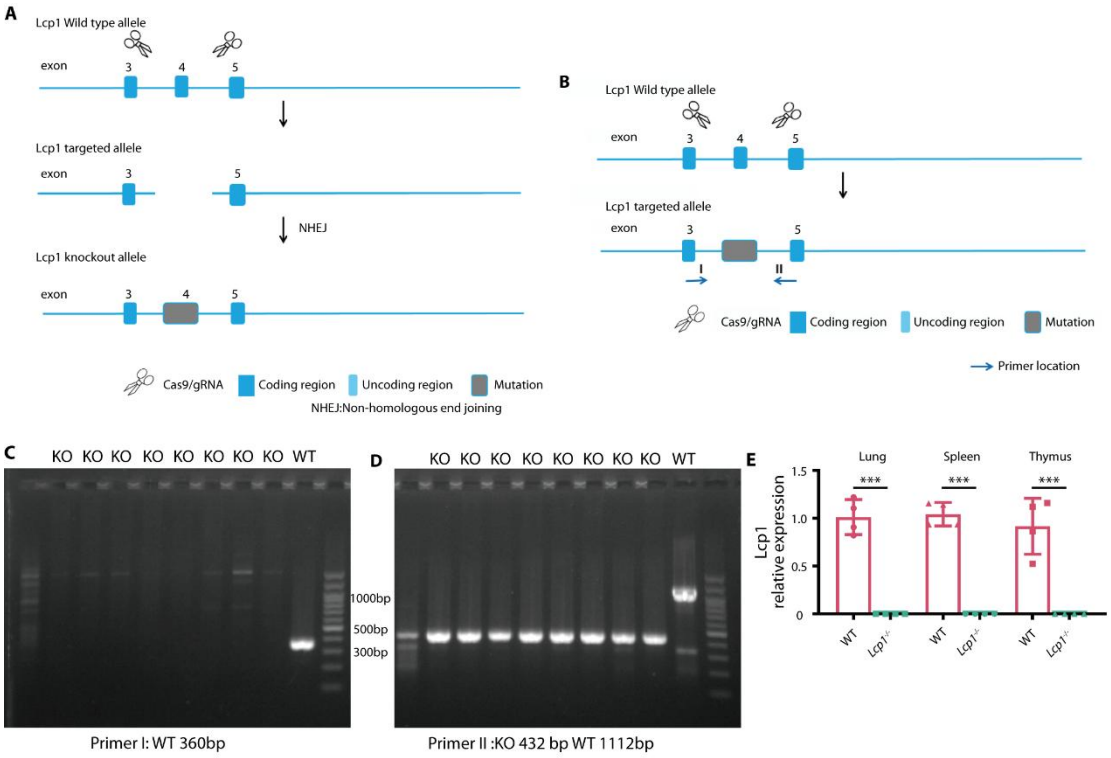

Fig. S2. *Lcp1* knockout strategy and verification.

(A) Using Cas9/gRNA to insert a mutated fragment in exon 4 of *Lcp1* gene to knockout *Lcp1* expression. **(B)** Description of genotyping primer location. **(C-D)** Genotyping gel imaging of *Lcp1* knockout mice and WT mice. **(E)** qPCR results of the mRNA level of *Lcp1* in lung, spleen, and thymus in wild type and *Lcp1* knockout mice. N=5 per group. *P < 0.05, **P < 0.01, and ***P < 0.001.

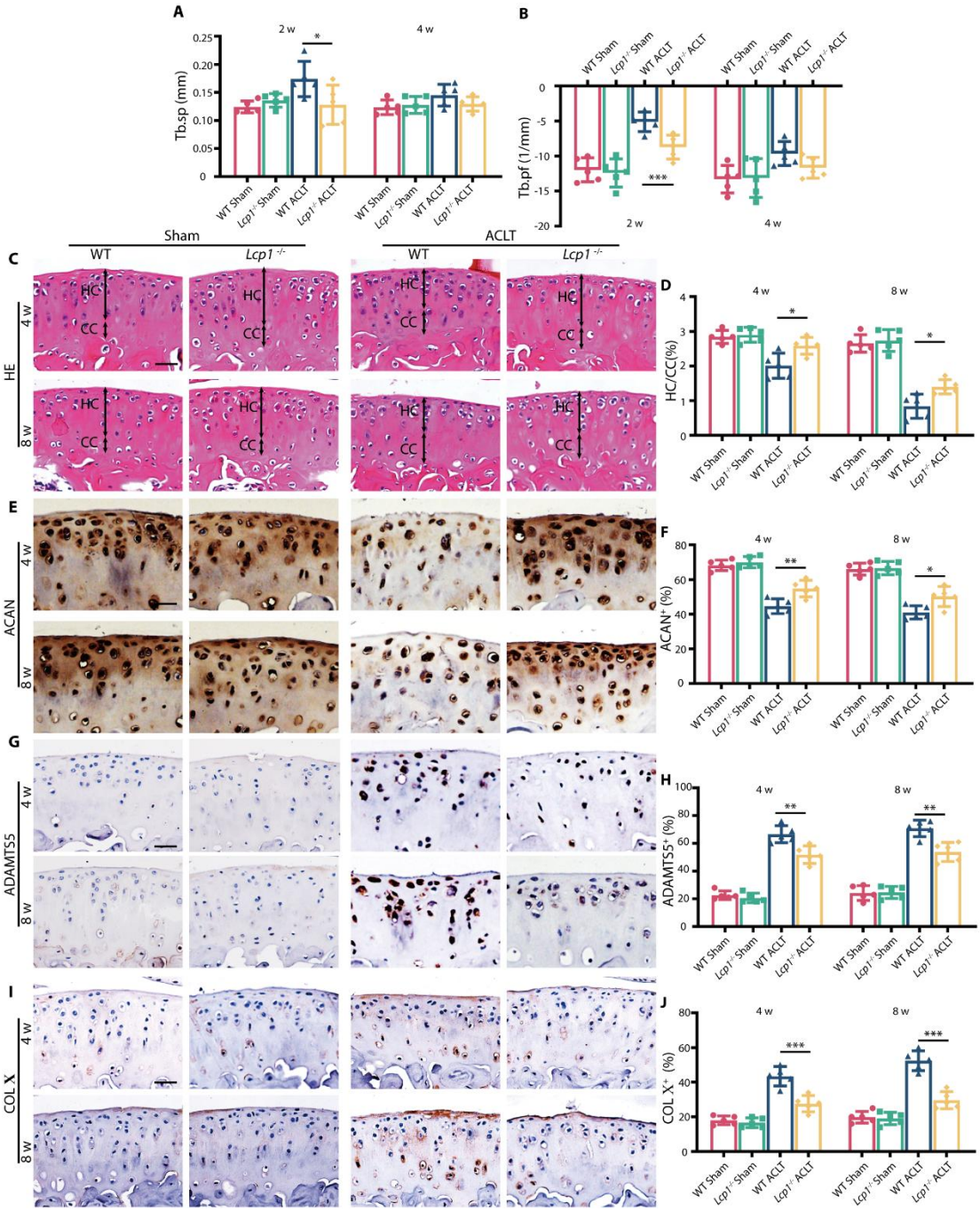

Fig. S3. Calcified cartilage duplication is retarded in *Lcp1* knockout mice.

(A) Micro-CT quantitative analysis of tibial subchondral bone trabecular spacing (Tb.sp, mm). **(B)** Micro-CT quantitative analysis of tibial subchondral bone trabecular bone pattern factor (Tb.pf, 1/mm). **(C)** Representative images of Hematoxylin and eosin staining of proximal tibia articular cartilage of *Lcp1*$^{-/-}$ mice and WT littermates at 4 and 8 weeks after ACLT. Double-headed arrows label range of HC and CC. Scale bar, 50 μm. **(D)** Ratio of HC and CC thickness. **(E)** Representative images of ACAN

immunohistochemistry in tibial articular cartilage of *Lcp1*$^{-/-}$ mice and WT littermates at 4 and 8 weeks after ACLT. Scale bar, 20 μm. **(F)** Quantitative analysis of ACAN positive area in articular cartilage. **(G)** Representative images of ADAMTS5 immunohistochemistry in tibial articular cartilage of *Lcp1*$^{-/-}$ mice and WT littermates at 4 and 8 weeks after ACLT. Scale bar, 20 μm. **(H)** Quantitative analysis of ADAMTS5 positive area in articular cartilage. **(I)** Representative images of COL X immunohistochemistry in tibial articular cartilage of *Lcp1*$^{-/-}$ mice and WT littermates at 4 and 8 weeks after ACLT. Scale bar, 20 μm. **(J)** Quantitative analysis of COL X positive area in articular cartilage. N=5 per group. *P < 0.05, **P < 0.01 and ***P < 0.001.

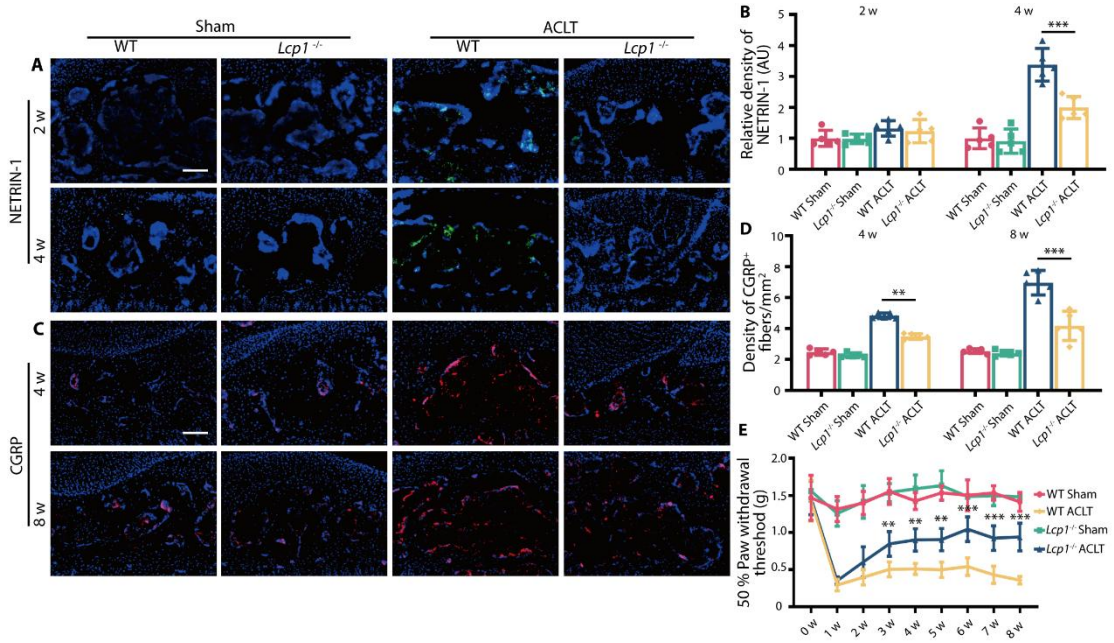

Fig. S4. *Lcp1* knockout mice show decreased NETRIN-1 and CGRP$^+$ sensory nerves in the subchondral bone and pain amelioration.

(A) Immunofluorescence staining of NETRIN-1 in *Lcp1*$^{-/-}$ and WT mouse tibial subchondral bone 2 and 4 weeks after ACLT. Scale bars, 100 μm. **(B)** Quantitative analysis of density of NETRIN-1 in subchondral bone marrow. **(C)** Immunofluorescence staining of CGRP$^+$ sensory nerve fibers in *Lcp1*$^{-/-}$ and WT mouse tibial subchondral bone 4 and 8 weeks after ACLT surgery. Scale bars, 100 μm. **(D)** Quantitative analysis of the density CGRP$^+$ nerve fibers in subchondral bone marrow. **(E)** Paw withdrawal threshold was tested at the right hind paw of *Lcp1*$^{-/-}$ and WT each week after surgery until 8 weeks. N=5 per group. *P < 0.05, **P < 0.01 and ***P < 0.001.

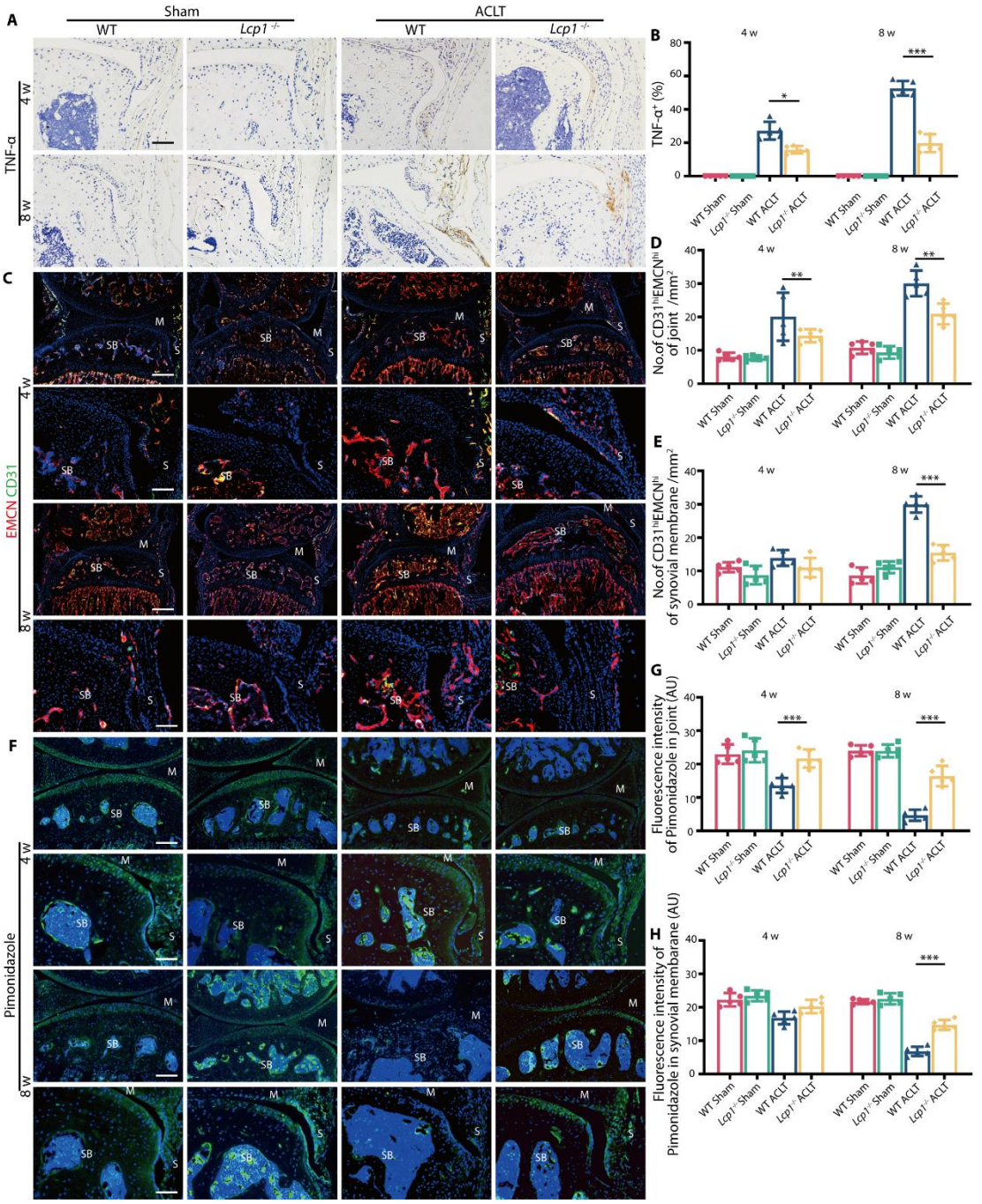

Fig. S5. Inflammation and angiogenesis in the whole joint.

(A) Representative images of TNF-α immunohistochemistry in synovium of *Lcp1*$^{-/-}$ mice and WT littermates at 4 and 8 weeks after ACLT. Scale bar, 20 μm. **(B)** Quantitative analysis of TNF-α positive area in synovial membrane. **(C)** Maximum intensity projections of immunostaining of EMCN (red), CD31 (green), and EmcnhiCD31hi (yellow) cells in knee joint and synovial membrane of *Lcp1*$^{-/-}$ mice

and WT mice at 4 and 8weeks post operation. Scale bar, 200 μm (1,3 raw), 50 μm (2,4 raw). **(D-E)** Quantification of CD31 and EMCN positive cells in knee joint (D) and synovial membrane (E). **(F)** Immunostaining of pimonidazole (green) in knee joint and synovial membrane of *Lcp1*$^{-/-}$ mice and WT mice at 4 and 8weeks post operation. Scale bar, 100 μm (1,3 raw), 50 μm (2,4 raw). **(G-H)** Quantification of pimonidazole fluorescence intensity in knee joint (G) and synovium (H). N=5 per group. *P < 0.05, **P < 0.01, and ***P < 0.001. M=meniscus, S=synovial membrane, SB=subchondral bone.

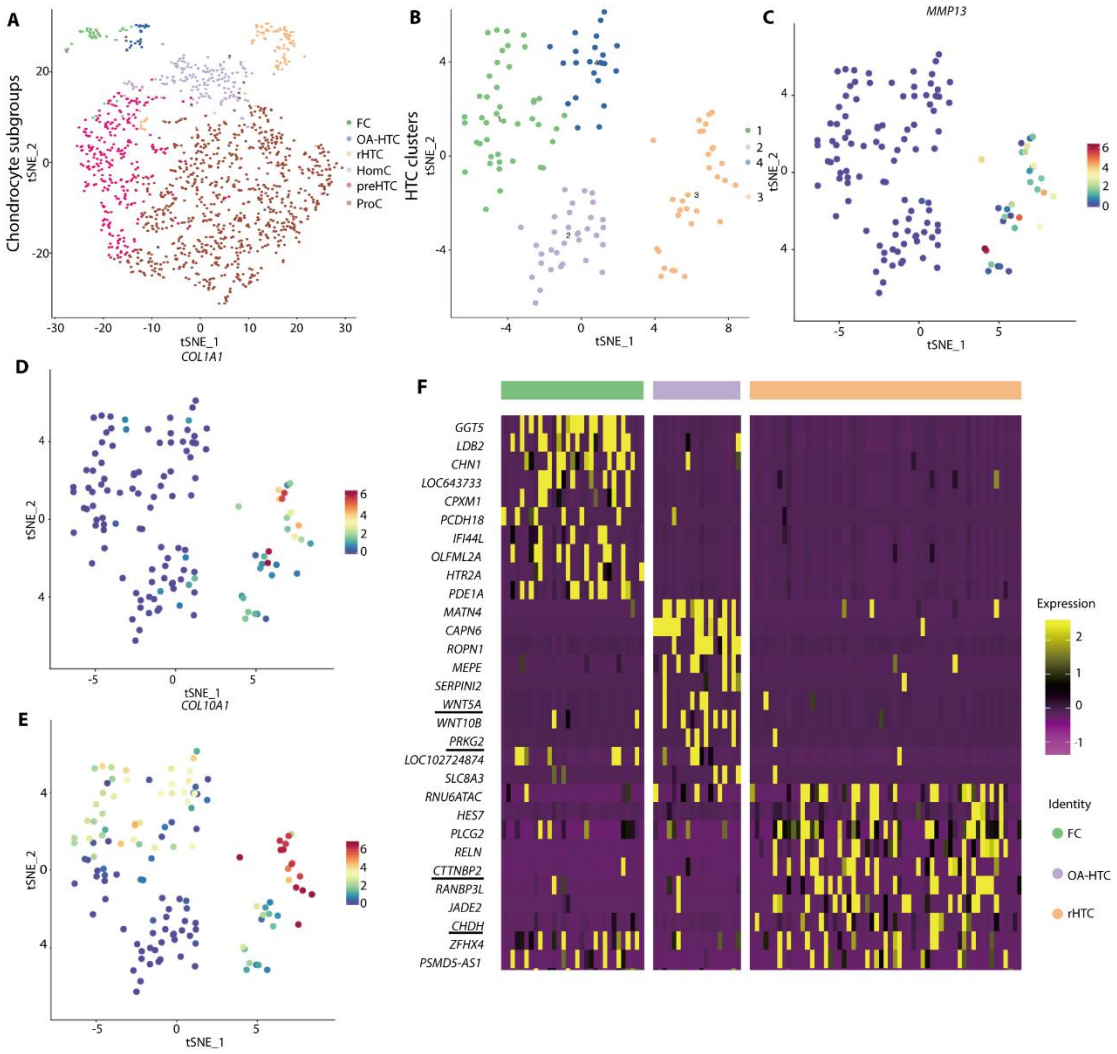

Fig. S6. HTC subsets definition and characteristics of OA-associated HTC.

(A) Visualization of t-SNE for different subsets of chondrocytes. **(B)** Visualization of t-SNE for different subsets of HTCs. **(C-E)** Dot plots showing the expression of *MMP13*, *COL1A1* and *COL10A1* of HTC subgroups. **(F)** Heatmap of top 10 different expression genes for FC, OA-HTC and rHTC.

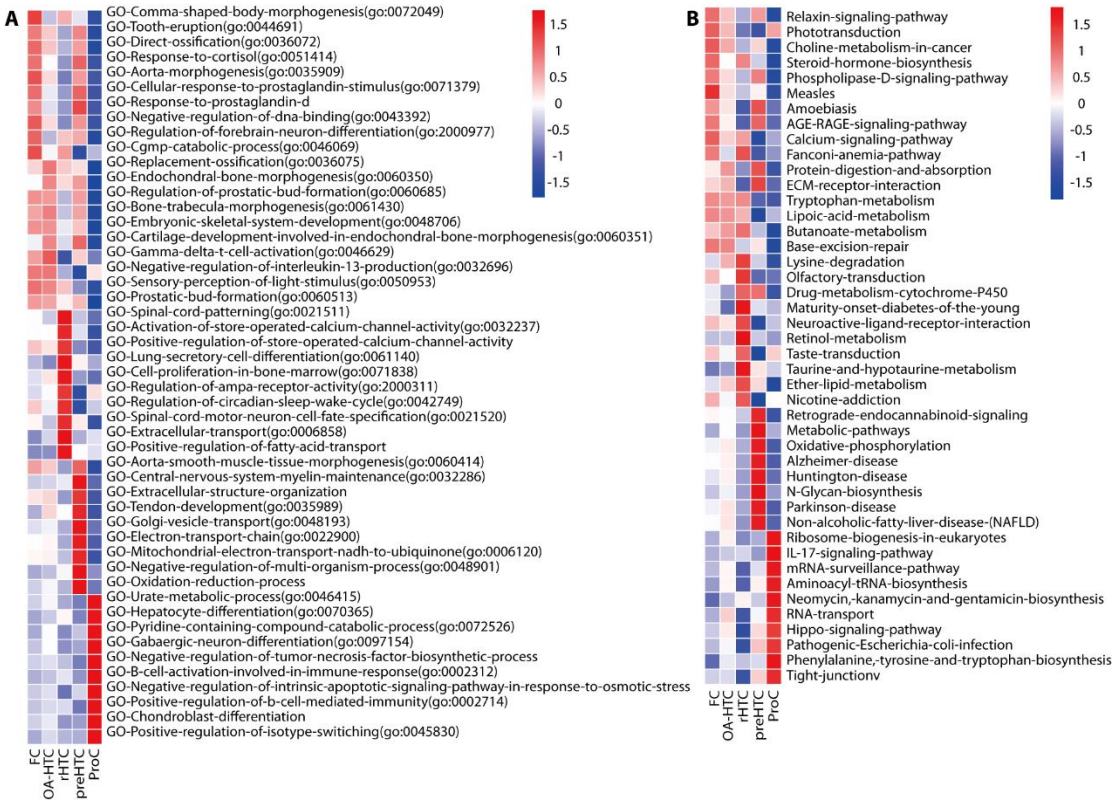

Fig. S7. KEGG and GO analysis of ProC, PreHTC, rHTC, OA-HTC and FC.

(A) Top 10 GO analysis result of FC, OA-HTC, rHTC, preHTC, and ProC.

(B) Top 10 KEGG pathway analysis result of FC, OA-HTC, rHTC, preHTC, and ProC.

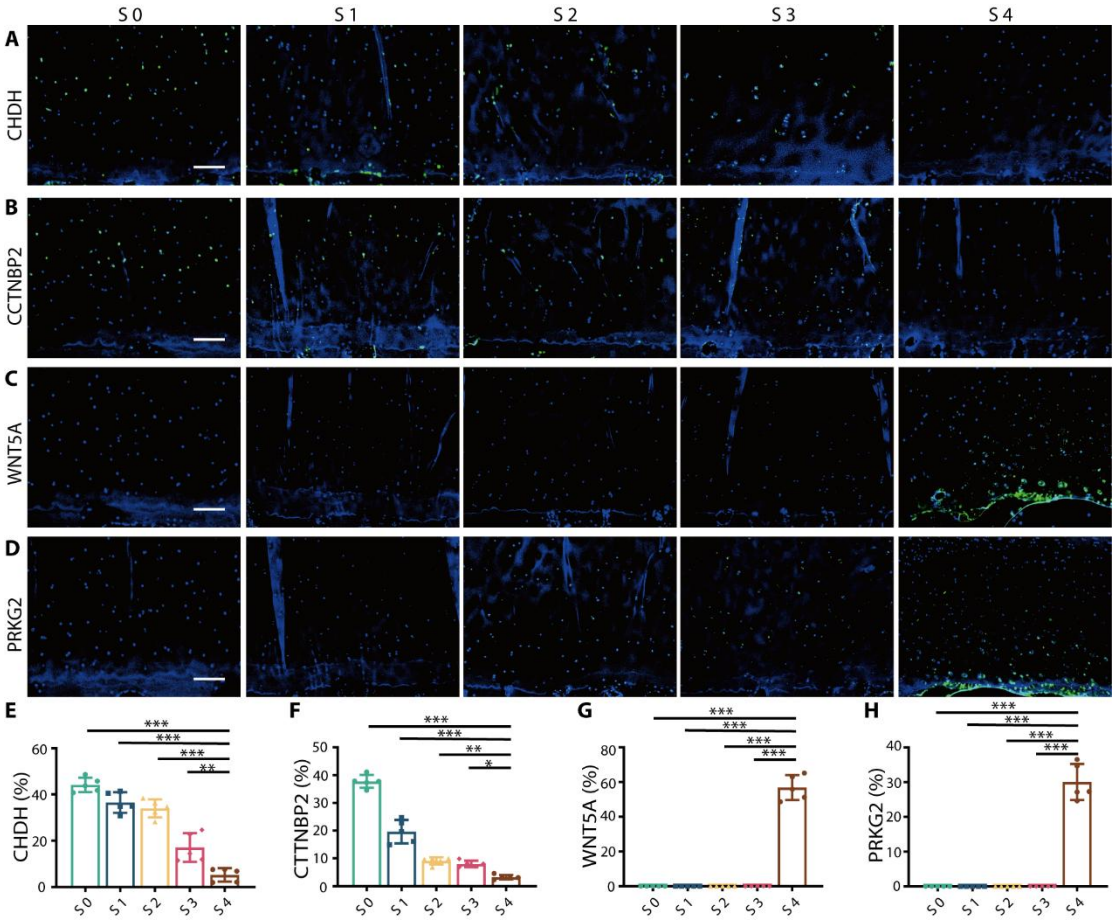

Fig. S8. HTC subsets verification in human samples.

(A-D) Immunofluorescence staining of CHDH, CTTNBP2, WNT5A, PRKG2 in different OARSI grade human tibia articular cartilage. Scale bar, 100 μm. **(E-H)** Quantitative analysis of CHDH, CTTNBP2, WNT5A, PRKG2 fluorescence positive area in human articular cartilage of different OARSI grade. N=5 per group. *P < 0.05, **P < 0.01, and ***P < 0.001.

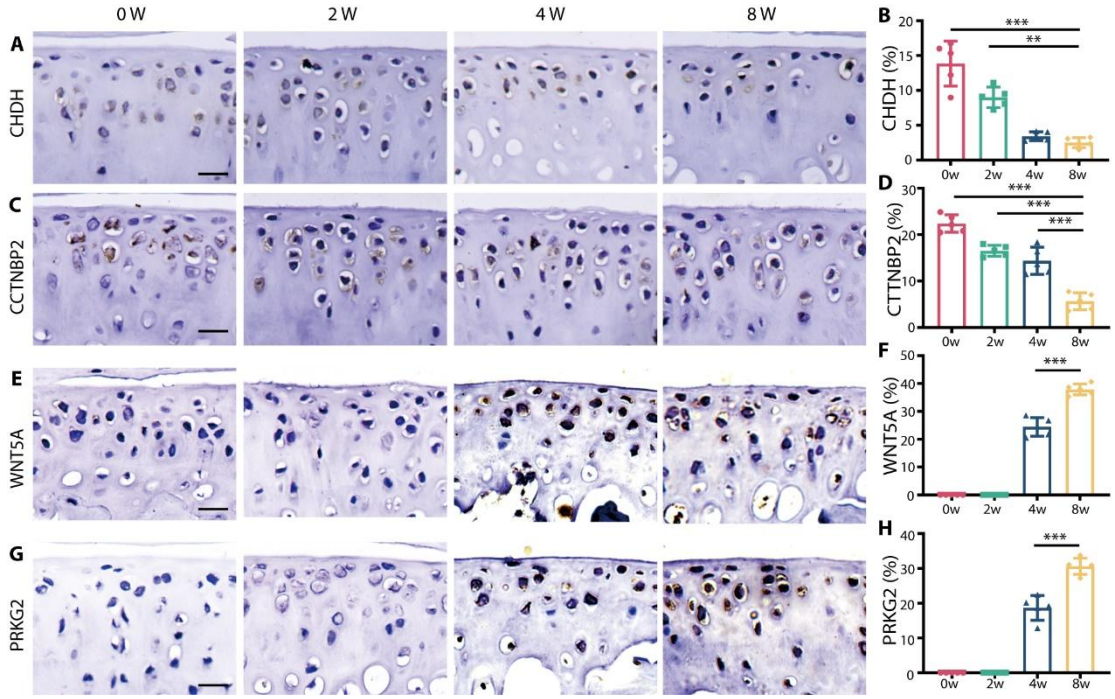

Fig. S9. HTC subsets verification in mouse samples.

(A) Representative images of CHDH immunohistochemistry in articular cartilage at 0,2,4 and 8 weeks after ACLT operation. Scale bar, 50 μm. **(B)** Quantitative analysis of CHDH positive area in articular cartilage. **(C)** Representative images of CTTNBP2 immunohistochemistry in articular cartilage at 0, 2, 4 and 8 weeks after ACLT operation. Scale bar, 50 μm. **(D)** Quantitative analysis of CTTNBP2 positive area in articular cartilage. **(E)** Representative images of WNT5A immunohistochemistry in articular cartilage at 0, 2, 4 and 8 weeks after ACLT operation. Scale bar, 50 μm. **(F)** Quantitative analysis of WNT5A positive area in articular cartilage. **(G)** Representative images of PRKG2 immunohistochemistry in articular cartilage at 0, 2, 4 and 8 weeks after ACLT operation. Scale bar, 50 μm. **(H)** Quantitative analysis of PRKG2 positive area in articular cartilage. N=5 per group. *P < 0.05, **P < 0.01, and ***P < 0.001.

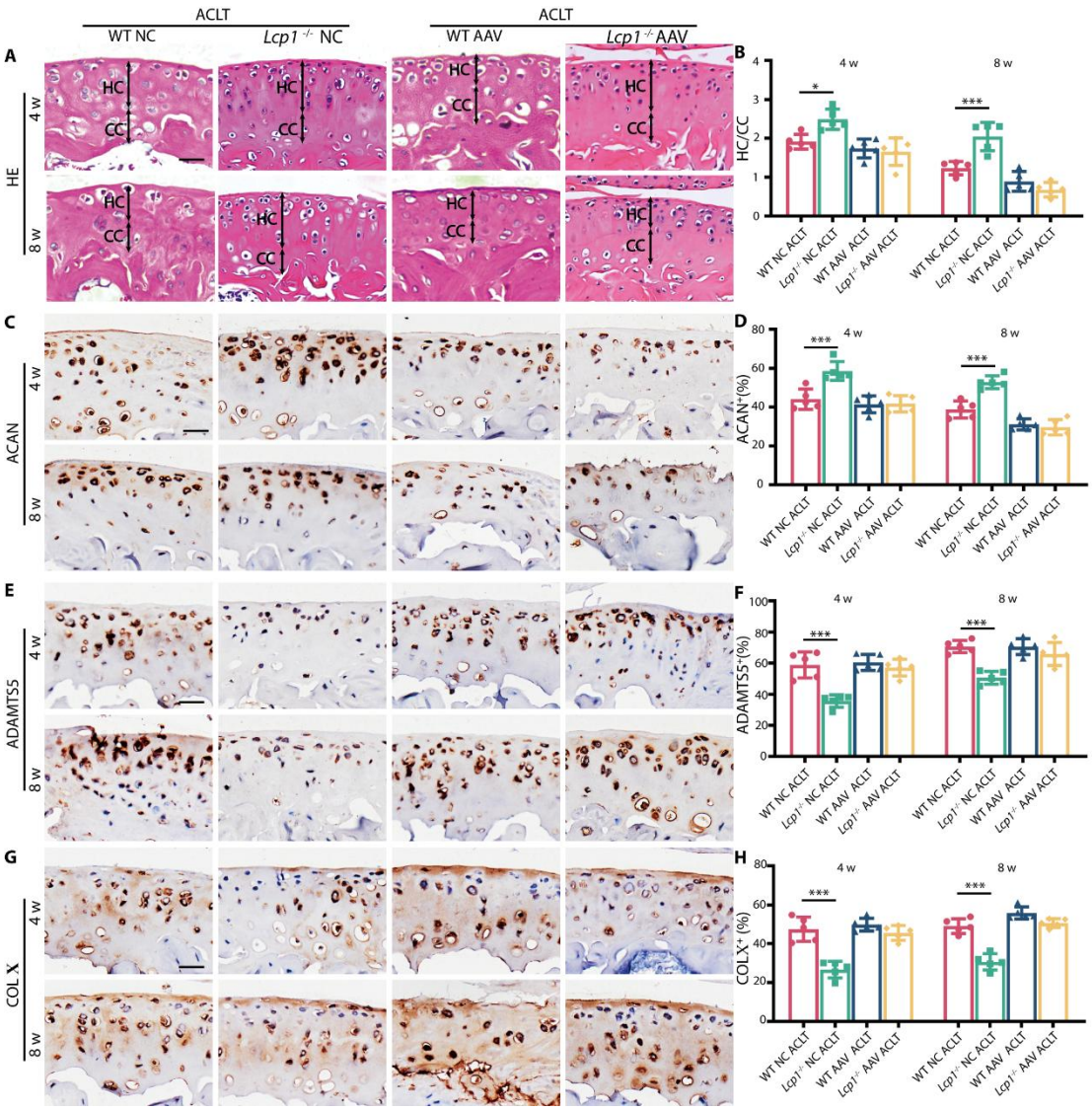

Fig. S10. Knockdown of *Hif1a* partially abolishes cartilage protection in *Lcp1*$^{-/-}$ mice.

(A) Representative images of hematoxylin and eosin staining of proximal tibia articular cartilage of *Lcp1*$^{-/-}$ and WT mice with *Hif1a* AAV or negative control at 4 and 8 weeks after ACLT. Double-headed arrows label range of HC and CC. Scale bar, 50 μm. **(B)** Ratio of HC and CC thickness. **(C)** Representative images of ACAN immunohistochemistry in tibial articular cartilage of *Lcp1*$^{-/-}$ and WT mice with *Hif1a* AAV or negative control at 4 and 8 weeks after ACLT. Scale bar, 20 μm. **(D)** Quantitative analysis of ACAN positive area in articular cartilage. **(E)** Representative

images of ADAMTS5 immunohistochemistry in tibial articular cartilage of *Lcp1*$^{-/-}$ and WT mice with *Hif1a* AAV or negative control at 4 and 8 weeks after ACLT. Scale bar, 20 μm. **(F)** Quantitative analysis of ADAMTS5 positive area in articular cartilage. **(G)** Representative images of COL X immunohistochemistry in tibial articular cartilage of *Lcp1*$^{-/-}$ and WT mice with *Hif1a* AAV or negative control at 4 and 8 weeks after ACLT. Scale bar, 20 μm. **(H)** Quantitative analysis of COL X positive area in articular cartilage. N=5 per group. *P < 0.05 **P < 0.01, and ***P < 0.001.

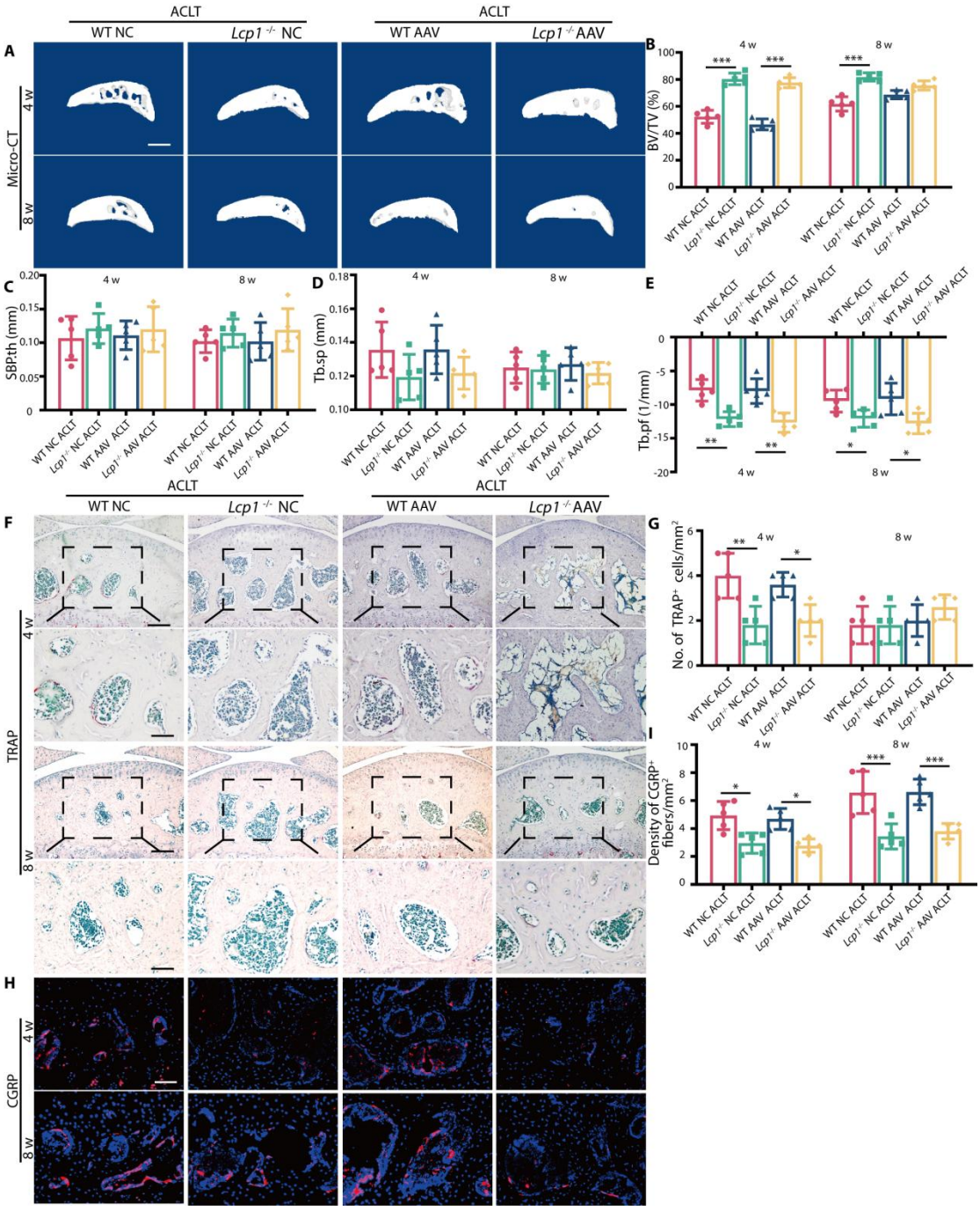

Fig. S11. Silencing *Hif1a* in cartilage does not affect subchondral bone in *Lcp1*$^{-/-}$ mice after ACLT.

(A) Representative Micro-CT 3D images of tibia subchondral bone of *Lcp1*$^{-/-}$ and WT mice with *Hif1a* AAV or negative control at 4 and 8 weeks after ACLT. Scale bar, 500 μm. **(B-E)** Micro-CT quantitative analysis of tibial subchondral bone, bone volume/tissue volume (BV/TV, %) (B), subchondral bone plate thickness (SBP. Th,

mm) (C), subchondral bone trabecular separation (Tb.sp, mm) (D) and subchondral bone trabecular bone pattern factor (Tb.pf) (E). **(F)** TRAP staining image of tibial subchondral bone of *Lcp1*$^{-/-}$ and WT mice with *Hif1a* AAV or negative control at 4 and 8 weeks after ACLT. Scale bar, 100μm (1,3 raw), 50 μm (2,4 raw). **(G)** Quantitative analysis of TRAP-positive cells in subchondral bone marrow. **(H)** Immunofluorescence staining of CGRP^{+} sensory nerve fibers of *Lcp1*$^{-/-}$ and WT mice with *Hif1a* AAV or negative control at 4 and 8 weeks after ACLT. Scale bar, 50 μm. **(I)** Quantitative analysis of the density CGRP^{+} nerve fibers in subchondral bone marrow. N=5 per group. *P < 0.05 **P < 0.01, and ***P < 0.001.

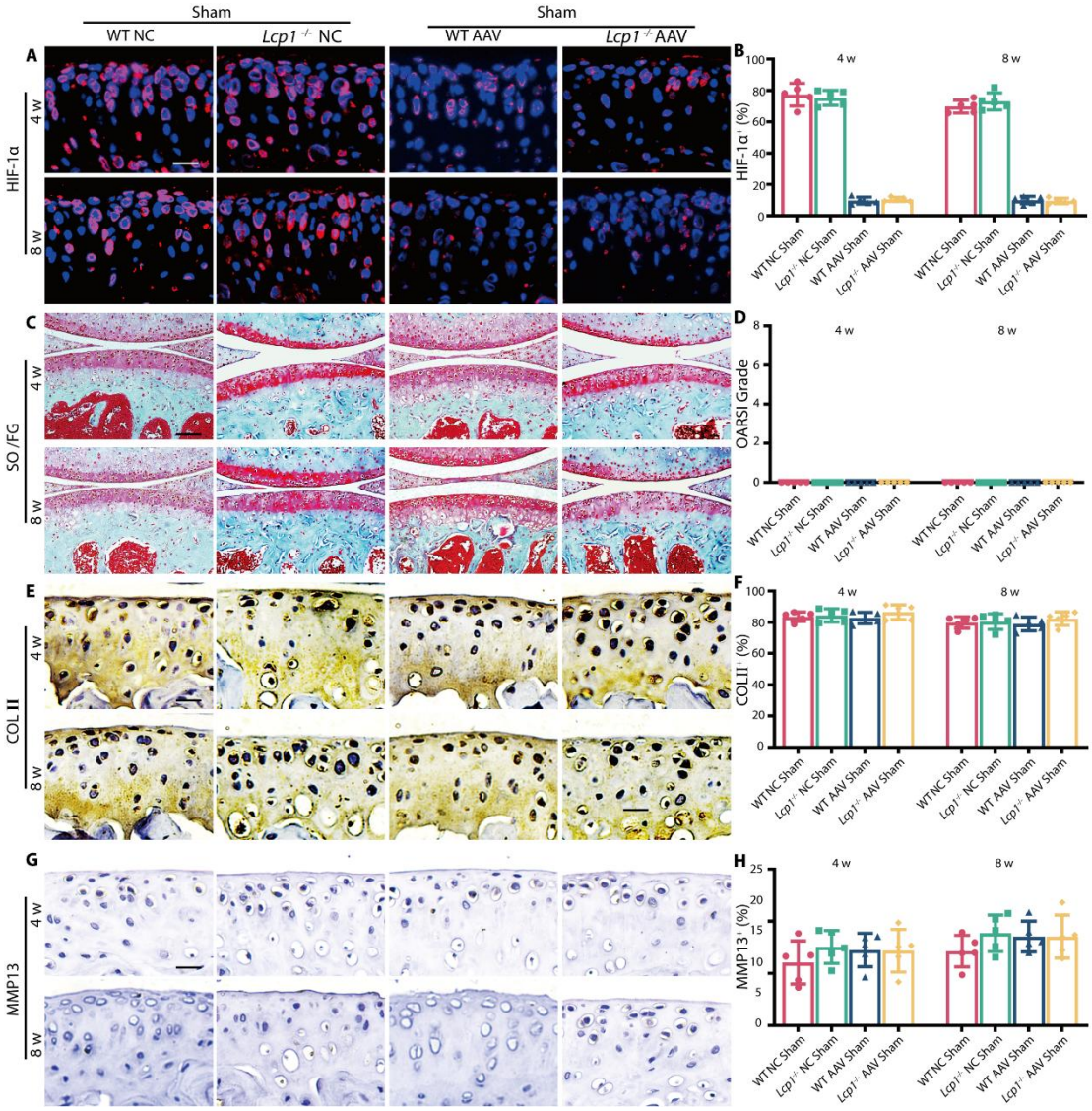

Fig. S12. Knockdown of *Hif1a* in sham mice has no effect on cartilage degeneration.

(A) Immunofluorescence staining of HIF-1α in tibial articular cartilage of *Lcp1*$^{-/-}$ and WT mice with *Hif1a* AAV or negative control AAV at 4 and 8 weeks after sham operation. Scale bar, 20 μm. **(B)** Quantitative analysis of HIF-1α immunofluorescence intensity of mice articular cartilage. **(C)** Knee articular cartilage safranin O/Fast Green staining of *Lcp1*$^{-/-}$ and WT mice with *Hif1a* AAV or negative control AAV at 4 and 8 weeks after sham operation. Scale bar, 100 μm. **(D)** OARSI grade of knee articular cartilage. (E) Representative images of COL II immunohistochemistry in articular

cartilage of *Lcp1*$^{-/-}$ and WT mice with *Hif1a* AAV or negative control at 4 and 8 weeks after sham operation. Scale bar, 20 μm. **(F)** Quantitative analysis of COL II positive area in articular cartilage. **(G)** Representative images of MMP13 immunohistochemistry in tibial articular cartilage of *Lcp1*$^{-/-}$ and WT mice with *Hif1a* AAV or negative control at 4 and 8 weeks after sham operation. Scale bar, 20 μm. **(H)** Quantitative analysis of MMP13 positive area in articular cartilage. N=5 per group. *P < 0.05, **P < 0.01, and ***P < 0.001.

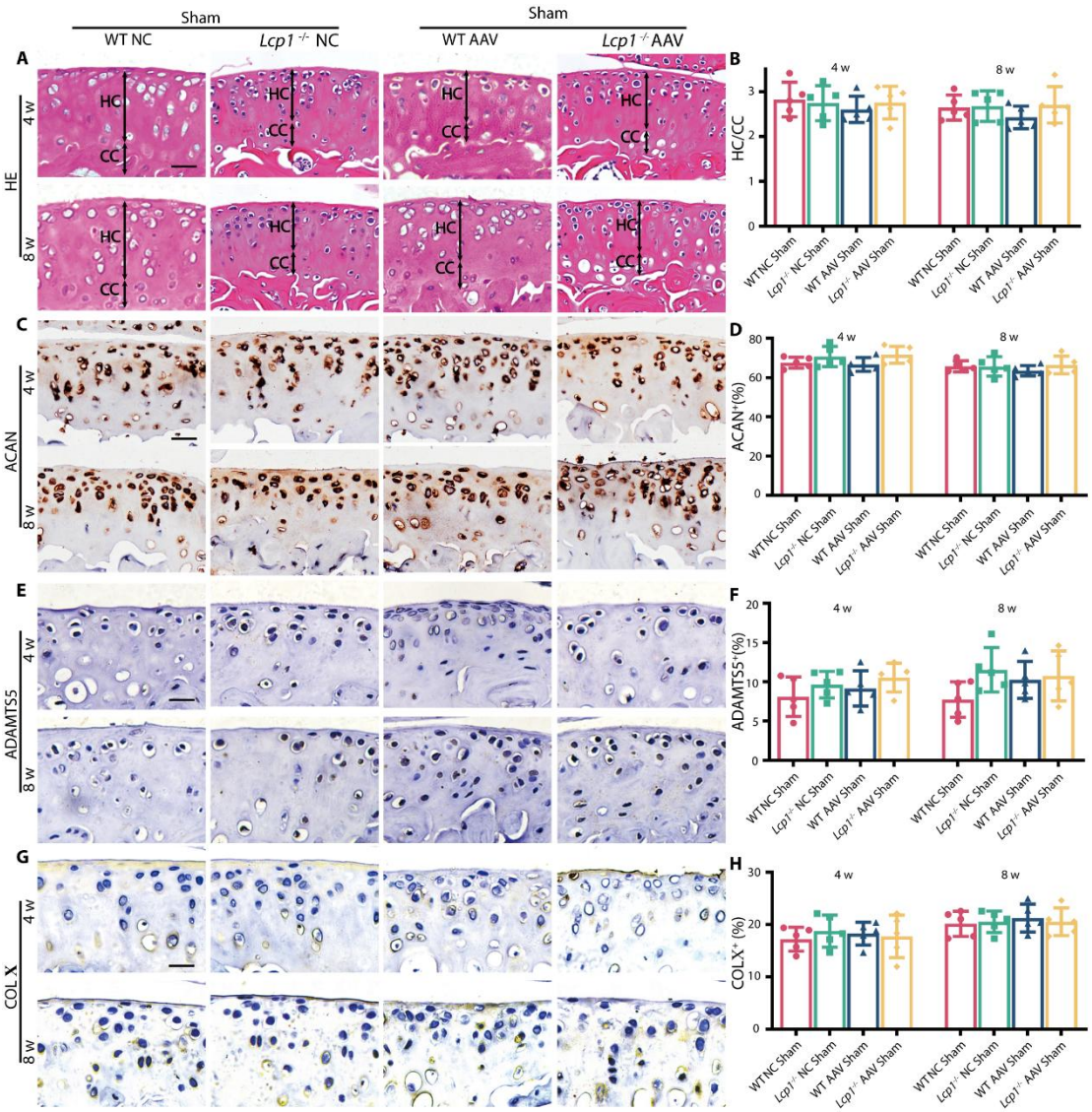

Fig. S13. Knockdown of *Hif1a* in sham mice has no effect on cartilage calcification.

(A) Representative images of Hematoxylin and eosin staining of proximal tibia articular cartilage of *Lcp1*$^{-/-}$ and WT mice with *Hif1a* AAV or negative control at 4 and 8 weeks after sham operation. Double-headed arrows label range of HC and CC. Scale bar, 50 μm. **(B)** Ratio of HC and CC thickness. **(C)** Representative images of ACAN immunohistochemistry in tibial articular cartilage of *Lcp1*$^{-/-}$ and WT mice with *Hif1a* AAV or negative control at 4 and 8 weeks after sham operation. Scale bar, 20

μm. **(D)** Quantitative analysis of ACAN positive area in articular cartilage. **(E)** Representative immunohistochemical staining of ADAMTS5 immunohistochemistry in tibial articular cartilage of *Lcp1*$^{-/-}$ and WT mice with *Hif1a* AAV or negative control at 4 and 8 weeks after sham operation. Scale bar, 20 μm. **(F)** Quantitative analysis of ADAMTS5 positive area in articular cartilage. **(G)** Representative images of COL X immunohistochemistry in tibial articular cartilage of *Lcp1*$^{-/-}$ and WT mice with *Hif1a* AAV or negative control at 4 and 8 weeks after sham operation. Scale bar, 20 μm. **(H)** Quantitative analysis of COL X positive area in articular cartilage. N=5 per group. *P < 0.05, **P < 0.01, and ***P < 0.001.

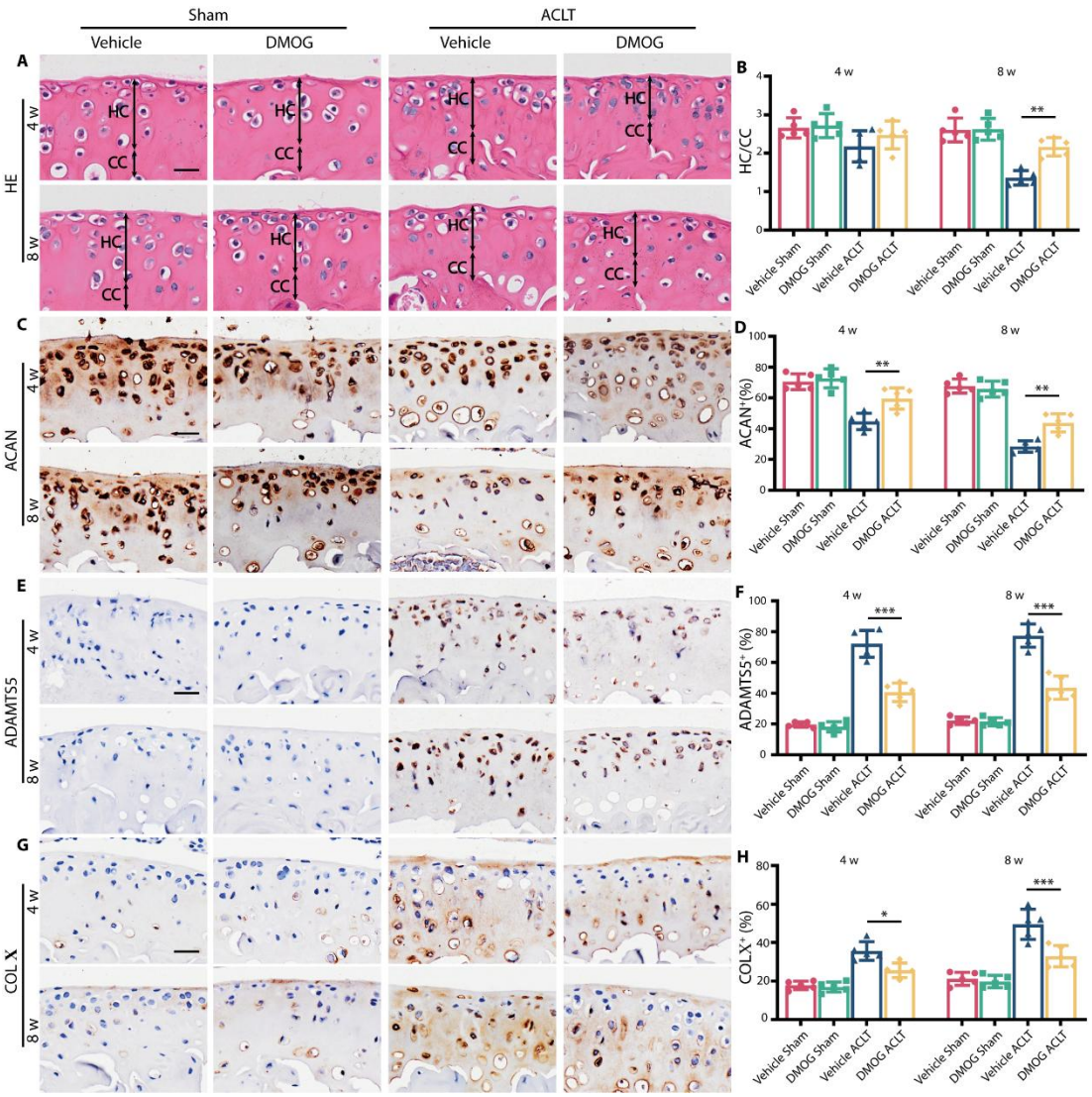

Fig. S14. DMOG prevents cartilage degeneration.

(A) Representative images of Hematoxylin and eosin staining of proximal tibia articular cartilage of WT mice with DMOG or normal saline at 4 and 8 weeks after ACLT. Double-headed arrows label range of HC and CC. Scale bar, 50 μm. **(B)** Ratio of HC and CC thickness. **(C)** Representative images of ACAN immunohistochemistry in tibial articular cartilage of WT mice with DMOG or normal saline at 4 and 8 weeks after ACLT. Scale bar, 20 μm. **(D)** Quantitative analysis of ACAN positive area in articular cartilage. **(E)** Representative images of ADAMTS5 immunohistochemistry in tibial articular cartilage of WT mice with DMOG or normal saline at 4 and 8 weeks

after ACLT. Scale bar, 20 μm. **(F)** Quantitative analysis of ADAMTS5 positive area in articular cartilage. **(G)** Representative images of COL X immunohistochemistry in tibial articular cartilage of WT mice with DMOG or normal saline at 4 and 8 weeks after ACLT. Scale bar, 20 μm. **(H)** Quantitative analysis of COL X positive area in articular cartilage. N=5 per group. *P < 0.05, **P < 0.01, and ***P < 0.001.

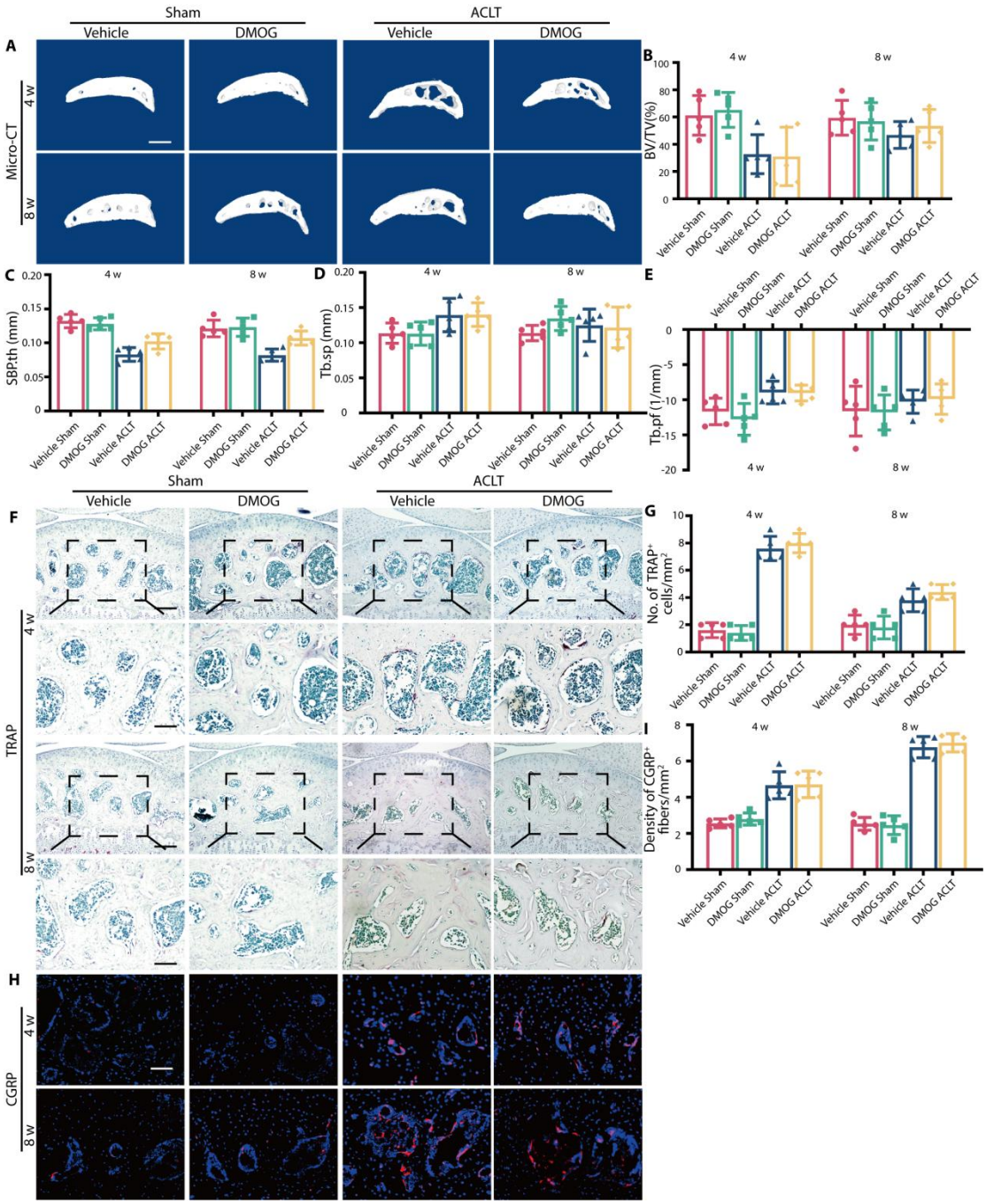

Fig. S15. DMOG does not affect subchondral bone in OA.

(A) Representative Micro-CT 3D images of tibia subchondral bone of WT mice with DMOG or normal saline at 4 and 8 weeks after ACLT. Scale bar, 500 μm. **(B-E)** Micro-CT quantitative analysis of tibial subchondral bone, bone volume/tissue volume (BV/TV, %) (B), subchondral bone plate thickness (SBP. Th, mm) (C), subchondral bone trabecular separation (Tb.sp, mm) (D) and subchondral bone

trabecular bone pattern factor (Tb.pf) (E). **(F)** TRAP staining image of tibial subchondral bone of WT mice with DMOG or normal saline at 4 and 8 weeks after ACLT. Scale bar, 100 μm (1,3 raw), 50 μm (2,4 raw). **(G)** Quantitative analysis of TRAP-positive cells in subchondral bone marrow. **(H)** Immunofluorescence staining of $CGRP^+$ sensory nerve fibers of WT mice with DMOG or normal saline at 4 and 8 weeks after ACLT. Scale bar, 50 μm. **(I)** Quantitative analysis of the density $CGRP^+$ nerve fibers in subchondral bone marrow. N=5 per group. *P < 0.05, **P < 0.01, and ***P < 0.001.

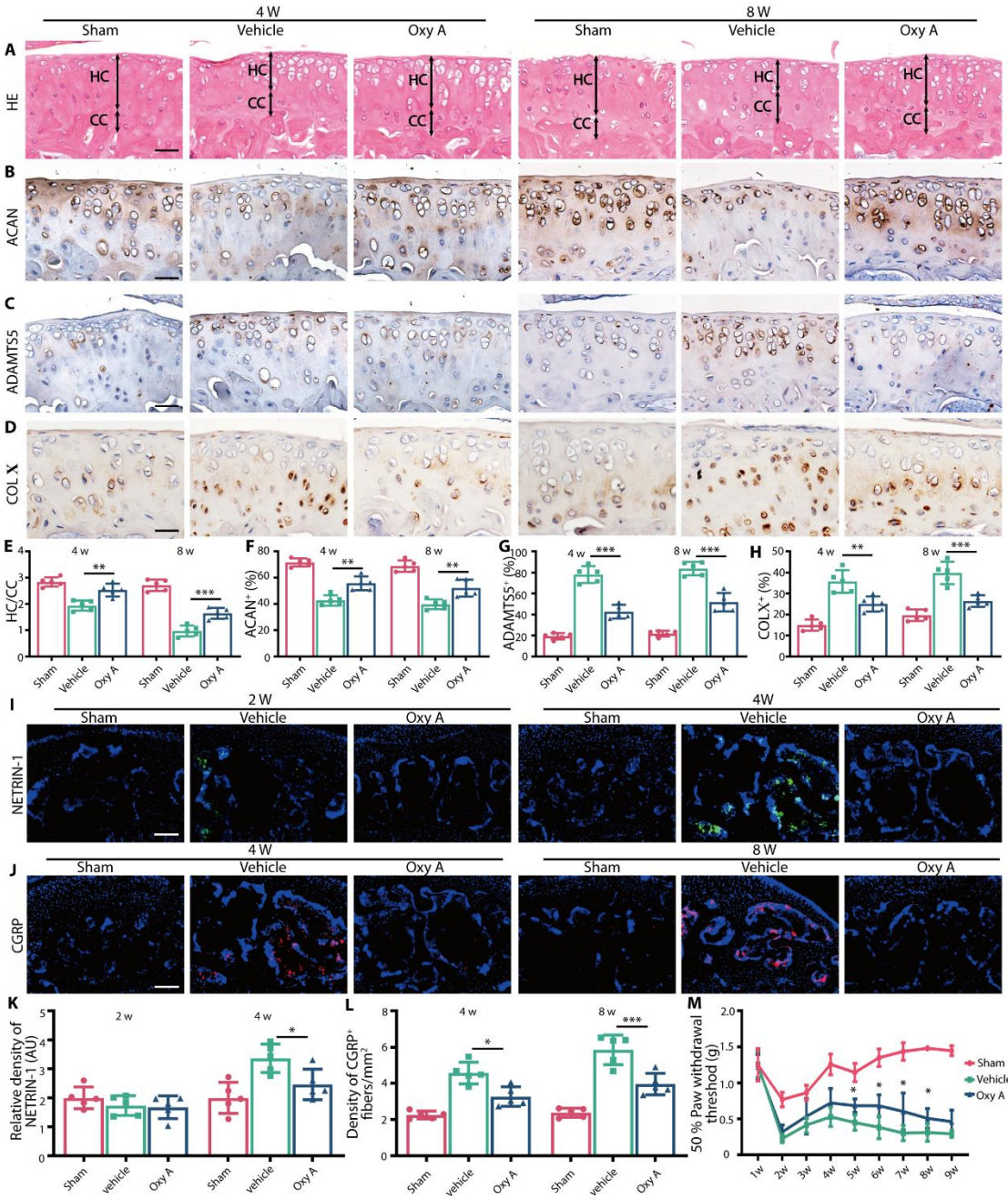

Fig. S16. Calcified cartilage duplication and sensory nerves innervation are retarded after Oroxylin A injection.

(A) Representative images of Hematoxylin and eosin staining of proximal tibia articular cartilage of WT mice with Oxy A or normal saline at 4 and 8 weeks after ACLT. Double-headed arrows label range of HC and CC. Scale bar, 50 μm. **(B)** Representative images of ACAN immunohistochemistry in tibial articular cartilage of

WT mice with Oxy A or normal saline at 4 and 8 weeks after ACLT. Scale bar, 20 μm. **(C)** Representative images of ADAMTS5 immunohistochemistry in tibial articular cartilage of WT mice with Oxy A or normal saline at 4 and 8 weeks after ACLT. Scale bar, 20 μm. **(D)** Representative images of COL X immunohistochemistry in tibial articular cartilage of WT mice with Oxy A or normal saline at 4 and 8 weeks after ACLT. Scale bar, 20 μm. **(E)** Ratio of HC and CC thickness. **(F)** Quantitative analysis of ACAN positive area in articular cartilage. **(G)** Quantitative analysis of ADAMTS5 positive area in articular cartilage. **(H)** Quantitative analysis of COL X positive area in articular cartilage. N=5 per group. **(I)** Immunofluorescence staining of NETRIN-1 in WT mice with Oxy A or normal saline at 2 and 4 weeks after ACLT. Scale bar, 100 μm. **(J)** Immunofluorescence staining of $CGRP^+$ sensory nerve fibers in WT mice with Oxy A or normal saline at 4 and 8 weeks after ACLT surgery. Scale bar, 100 μm. **(K)** Quantitative analysis of density of NERTIN-1 in subchondral bone marrow. **(L)** Quantitative analysis of the density $CGRP^+$ nerve fibers in subchondral bone marrow. **(M)** Paw withdrawal threshold was tested at the right hind paw of WT mice with Oxy A or normal saline each week after surgery until 8 weeks. N=5 per group. *$P < 0.05$, **$P < 0.01$, and ***$P < 0.001$.

Movies S1 Video of ^{18}F-FMISO PETCT in *Lcp1*$^{-/-}$ mice 4 weeks after ACLT

Movies S2 Video of ^{18}F-FMISO PETCT in WT mice 4 weeks after ACLT